

Weak Decay of ${}^{12}_{\Lambda}\text{C}$ and ${}^{11}_{\Lambda}\text{B}$ Hypernuclei

R. Grace, P. D. Barnes, R. A. Eisenstein,^(a) G. B. Franklin, C. Maher, R. Rieder, J. Seydoux,
J. Szymanski, and W. Wharton^(b)

Carnegie-Mellon University, Pittsburgh, Pennsylvania 15213

and

S. Bart, R. E. Chrien, P. Pile, and Y. Xu

Brookhaven National Laboratory, Upton, New York 11973

and

R. Hackenburg and E. Hungerford

University of Houston, Houston, Texas 77004

and

B. Bassalleck

University of New Mexico, Albuquerque, New Mexico 87131

and

M. Barlett and E. C. Milner

University of Texas, Austin, Texas 78712

and

R. L. Stearns

Vassar College, Poughkeepsie, New York 12601

(Received 9 May 1985)

A measurement is reported of the mean lifetime, τ , for the weak decay of ${}^{12}_{\Lambda}\text{C}$ and ${}^{11}_{\Lambda}\text{B}$ hypernuclei. The experiment detected energetic protons from the hypernuclear nonmesonic decay $\Lambda + p \rightarrow n + p$, in coincidence with hypernuclear production by the strangeness-changing reactions ${}^{12}\text{C}(K^-, \pi^-){}^{12}_{\Lambda}\text{C}$ and ${}^{12}\text{C}(K^-, \pi^-)p, {}^{11}_{\Lambda}\text{B}$. The measured ground-state decay lifetimes $\tau({}^{12}_{\Lambda}\text{C}) = (2.11 \pm 0.31) \times 10^{-10}$ sec and $\tau({}^{11}_{\Lambda}\text{B}) = (1.92 \pm 0.22) \times 10^{-10}$ sec are compared with ΛN weak-interaction calculations.

PACS numbers: 21.80.+a, 13.75.Ev, 14.20.Jn, 21.30.+y

A lambda hyperon bound to a nucleus will decay with a lifetime typical of weak processes ($\sim 10^{-10}$ sec). This is long compared to the normal strong and electromagnetic (strangeness-conserving) nuclear decay processes so that one generally expects the strangeness-changing decay process to occur for a Λ in the lowest (1S) nuclear shell-model orbital. This weak interaction is characterized by a total decay rate which equals the sum of four partial rates:

$$\Gamma_{\text{total}} = 1/\tau = \Gamma_m(\pi^-) + \Gamma_m(\pi^0) + \Gamma_{\text{nm}}(p) + \Gamma_{\text{nm}}(n).$$

Here the four respective decay branches and decay rates are the mesonic decays giving π^- ,

$$\Lambda \rightarrow p + \pi^-, \quad Q = 38 \text{ MeV} - (B_{\Lambda} - B_p),$$

and π^0 ,

$$\Lambda \rightarrow n + \pi^0, \quad Q = 41 \text{ MeV} - (B_{\Lambda} - B_n);$$

and the nonmesonic decays giving a proton,

$$\Lambda + p \rightarrow n + p, \quad Q = 177 \text{ MeV} - (B_{\Lambda} + B_p),$$

and only neutrons,

$$\Lambda + n \rightarrow n + n, \quad Q = 176 \text{ MeV} - (B_{\Lambda} + B_n),$$

where B_b is the binding energy for baryon b .

The mesonic decay branches are analogous to the decay of a free lambda. The nonmesonic decays, on the other hand, are more closely related to NN parity-nonconserving forces. This relationship is clearly demonstrated when one views these interactions as taking place by the exchange of a single meson from a weak vertex (Fig. 1). A measurement of these *nonmesonic* decay rates is the primary objective of the experiment described below. We report here the measurement of the mean lifetime, τ , which is dominated by Γ_{nm} .

The ratio of the mesonic and nonmesonic rates is expected to vary as a function of hypernuclear mass. For the very light hypernuclei ($A = 3, 4$) the mesonic decay modes are favored, while for heavier hypernuclei, the nonmesonic rates dominate. The reasons for this trend are threefold¹: (1) The increased binding of the lambda in heavier hypernuclei sharply restricts the

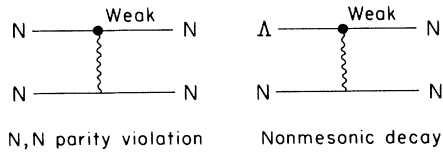


FIG. 1. Comparison of NN parity-nonconserving (“violating”) interaction and the ΛN nonmesonic decay process, assuming the interaction takes place via single meson exchange.

phase space available to the mesonic decays. (2) The heavier nuclei have fewer available states for the slowly recoiling nucleon from the mesonic decay (Pauli blocking). (3) The increasing nuclear density of the heavier hypernuclei increases the overlap of the lambda-nucleon wave functions hence enhancing the nonmesonic rate.

Recent theoretical work²⁻⁷ has focused on the nonmesonic rates in infinite nuclear matter and in finite nuclei. Lifetime measurements exist¹ for hypernuclei in the region $A = 3-5$ and, as well, for $A = 16$ where a total of only 22 events above background were observed.⁸ A high-precision lifetime measurement in the region where the nonmesonic modes are expected to dominate is needed in order to test these calculations.

We report here an experiment to measure, for the first time, the lifetime of ${}^{12}_{\Lambda}\text{C}$, which was performed at the LESBI beam line^{9,10} at the Brookhaven alternating-gradient synchrotron (AGS). An 800-MeV/c kaon beam was incident on a 4-gm/cm²-thick target of scintillator material (CH). The strangeness-changing reaction $K^- + {}^{12}\text{C} \rightarrow {}^{12}_{\Lambda}\text{C} + \pi^-$ was used for hypernuclear formation and tagging. Detection and momentum analysis of the π^- emitted at 6° relative to the K^- beam direction permitted generation of the ${}^{12}_{\Lambda}\text{C}$ mass spectrum (see Fig. 2) and thus provided a tag for ${}^{12}_{\Lambda}\text{C}$ hypernuclear production. The choice of ${}^{12}_{\Lambda}\text{C}$ as a hypernuclear system for study was motivated by a previous measurement¹¹ which reported that the nonmesonic rate is a factor of 5 larger than the π^- mesonic rate [$\Gamma_{nm}/\Gamma_m(\pi^-) = 5$] and thus dominates the weak decay process.

The charged decay products of the tagged hypernuclei were detected in a scintillator range spectrometer, shown in Fig. 3, which was positioned directly below the hypernuclear production target. It consisted of fifteen slabs of scintillator material, and a multiwire proportional chamber with two pairs of orthogonal planes. The first two scintillators, which were positioned on opposite faces of the wire chamber, were high-quality timing counters used in the time measurement of the decay process. The next twelve elements were used in the energy measurement. The last counter was used to veto particles that passed through the range spectrometer, which encompassed a solid angle of about $\Delta\Omega = 1.5$ sr.

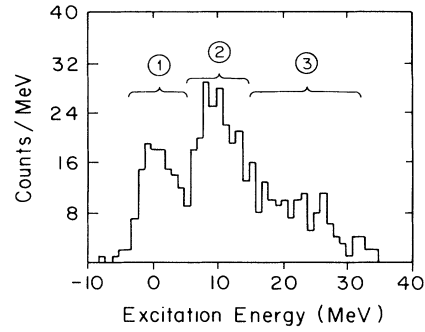


FIG. 2. The ${}^{12}_{\Lambda}\text{C}$ hypernuclear excitation-energy spectrum with experimental cuts shown for each of the three states discussed in the text.

In the ${}^{12}_{\Lambda}\text{C}$ mass spectrum, three hypernuclear states were observed in coincidence with energetic protons from nonmesonic decay: the hypernuclear ground state and two excited states (Fig. 2). Note that the excited hypernuclear states are not bound and may decay strongly by nucleon emission to a lighter hypernucleus or by free-lambda emission. However, because the low-energy proton (5 MeV) from the free-lambda decay is below our detection threshold of 30 MeV, free-lambda decay does not contribute to the mass spectrum. Since these energetic protons were detected in coincidence with the production of an unbound hypernuclear state, this state must ultimately have decayed to a stable hypernucleus.

The following is a discussion of the three hypernuclear states observed in this experiment. The ground state of the nucleus ${}^{12}_{\Lambda}\text{C}$ (region 1 in Fig. 2), which has been observed in angular distribution studies of the ${}^{12}\text{C}(K, \pi)$ reaction,¹¹ is interpreted as the particle-hole shell-model configuration $[s(\Lambda), p^{-1}(n)]$, and is bound by about 11 MeV. The first excited state (region 2 in Fig. 2) has the configuration¹¹ $[p(\Lambda), p^{-1}(n)]$, and is 3 MeV above the ${}^{11}_{\Lambda}\text{B} + p$ breakup threshold. This state has been observed to decay strongly¹² to ${}^{11}_{\Lambda}\text{B}$ plus a low-energy proton. Therefore, hypernuclear decays detected in coincidence with this state are associated with ${}^{11}_{\Lambda}\text{B}$ (and not ${}^{12}_{\Lambda}\text{C}$) plus a low-energy proton that stops in the target. The third state

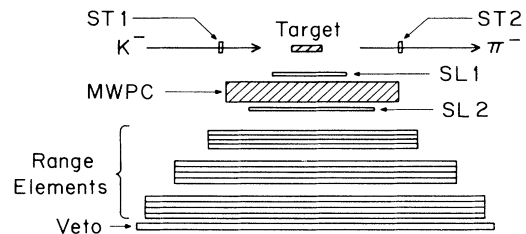


FIG. 3. Schematic view of the range spectrometer used in the hypernuclear lifetime measurement. The pion magnetic spectrometer is out of the figure to the right.

(region 3 in Fig. 2) is unbound by 10 MeV, and is tentatively identified¹³ as having the shell-model configuration $[s(\Lambda), s^{-1}(n)]$ which is expected to occur at an excitation energy of about 20 MeV and to be about 9–10 MeV wide. Although the exact mode of the strong breakup of this state is unknown, the detection here of energetic protons associated with this state establishes that this breakup produces a stable hypernucleus.

The lifetime was measured by determining the hypernuclear production time (t_p) and the hypernuclear decay time (t_d) for each event, and calculating the difference ($t_d - t_p$). The product time was obtained from the redundant pair of scintillators (ST1,ST2) in the beam corrected for the flight time of the beam particle from the scintillator to the target. The decay time was determined by the first two scintillators (SL1,SL2) in the range spectrometer plus a correction for the flight time of the decay proton from the target to the respective scintillator. The energy of the proton and the angle of the proton's trajectory, measured with the range spectrometer, were used to compute the flight-time corrections. Identification of protons in the range spectrometer was accomplished by use of both the measured range and the energy-loss information. We estimate that less than 2% of our proton sample is contaminated by misidentified pions.

An important component of this measurement was the use of the reaction $\pi^- + {}^{12}\text{C} \rightarrow X + p$ to provide a monitor for the prompt-time resolution shape, $R(t)$. Since the beam contained roughly ten pions for each kaon we were able to collect these events simultaneously with the hypernuclear-decay events. The prompt spectrum obtained in this measurement was Gaussian in shape with $\sigma = 140$ psec. This resolution includes contributions from the flight-time corrections as well as the intrinsic resolution of the counters.

The protons from the hypernuclear decay are distributed in time according to the probability distribution

$$P(t) = (1/\tau)e^{-t/\tau},$$

where τ is the hypernuclear lifetime, and $P(t)$ is the instantaneous rate. The actual measured time distribution $S(t)$ is a convolution of $P(t)$ with the experimental resolution function $R(t)$:

$$S(t) = (1/N) \int R(u)P(t-u)du.$$

Notice that the first moments, M_1 , of the S , R , and P distributions are related by $M_1(S) = M_1(R) + M_1(P)$ such that the lifetime, $\tau = M_1(P)$, can be simply expressed as the mean shift of $S(t)$ with respect to $R(t)$, $\tau = M_1(S) - M_1(R)$. A measurement of a lifetime on the same order as σ by the mean-shift method is possible with an error of about $\pm 10\%$ for 200 decay events.

The combination of two beam scintillators (ST1,ST2) with two scintillators (SL1,SL2) in the range spectrometer can produce four time-of-flight distributions. These distributions are not independent since each one contains the same sample of decay events. They differ only with respect to fluctuations in the instrumentation response. However, these four distributions provide a consistency check. That is, they all give the same result within the statistical errors of the analysis.

Figure 4 shows the measured prompt distribution, $R(t)$, and one of the four distributions, $S(t)$, obtained for the first excited state. The prompt distribution contains 877 events and the lifetime distribution $S(t)$ contains 221 events.

The lifetime was determined for each of the four distributions for each state by fitting the data with the function $S(t)$ defined above. The fitting procedure used here was the usual χ^2 method of maximum likelihood but employed Poisson statistics and gave $\chi^2/\nu = 0.63$ for ν degrees of freedom. This method has been shown to yield improved results for fitting nuclear lifetimes.¹⁴

A final value for the lifetime for each state was obtained by a weighted average of the four values for each state. The results of the analysis are summarized in Table I. The errors quoted in Table I are statistical. Note that since the four distributions are not independent the errors are not related to the errors associated with the individual measurements in the usual way. Systematic errors can arise as a result of differences in the energy or angular distributions of the protons from the hypernuclear decay and those from the prompt reaction. The measured proton energy distributions are quite similar. This result, coupled with the absence of a detectable correlation between the measured distributions for $S(t)$ and for $R(t)$ with respect to the proton energy and angle distributions, strongly supports the conclusion that the systematic errors as-

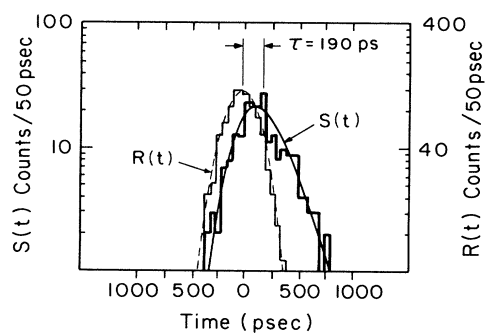


FIG. 4. The time distribution, $S(t)$, obtained from the decay of the ${}^{12}\text{C}$ first excited state (region 2, Fig. 2) compared to the prompt-timing distribution, $R(t)$, obtained from the reaction $\pi + {}^{12}\text{C} \rightarrow X + p$.

TABLE I. Results of the hypernuclear lifetime analysis. Values are listed for the lifetime (τ), the errors (σ), and the number of counts (N) in each distribution, for each of the three regions of Fig. 2 discussed in the text. All times are given in picoseconds.

Counters	$^{12}\Lambda\text{C}(0)$			$^{10}\Lambda\text{B}(0)$			$^A\Lambda\text{Z}$		
	τ	σ_τ	N	τ	σ_τ	N	τ	σ_τ	N
ST1,SL1	220	31	109	187	24	231	185	30	97
ST1,SL2	221	37	83	190	22	174	264	67	66
ST2,SL1	209	31	105	190	24	221	192	31	95
ST2,SL2	189	39	80	201	24	167	280	65	67
Average	211 \pm 31			192 \pm 22			201 \pm 30		

sociated with this measurement are small in comparison with statistical errors.

The final lifetime results (the last row of Table I) can be converted to decay rates and expressed as a ratio to the free-lambda decay rate, $\Gamma_\Lambda = 3.80 \times 10^9 \text{ sec}^{-1}$, as follows: state 1,

$$\Gamma(^{12}\Lambda\text{C})/\Gamma_\Lambda = 1.25 \pm 0.18;$$

state 2,

$$\Gamma(^{11}\Lambda\text{B})/\Gamma_\Lambda = 1.37 \pm 0.16;$$

state 3,

$$\Gamma(^A\Lambda\text{Z})/\Gamma_\Lambda = 1.31 \pm 0.20,$$

where $^A\Lambda\text{Z}$ represents the unknown final hypernucleus associated with state 3. To the extent that these total rates are dominated by the nonmesonic process they can be compared with the calculated nonmesonic decay rates for infinite nuclear matter obtained by McKellar and Gibson² ($\Gamma_{\text{nm}}/\Gamma_\Lambda = 0.5$ to 2.0), and for the hypernucleus $^{12}\Lambda\text{C}(0)$ obtained by Heddle and co-workers^{3,4} ($\Gamma_{\text{nm}}/\Gamma_\Lambda = 2.25$) in a hybrid quark model. Bandō and Tahaki⁶ obtain a total rate $\Gamma(^{12}\Lambda\text{C})/\Gamma_\Lambda = 1.13$, in a density-dependent Hartree-Fock calculation of the mesonic decay of $^{12}\Lambda\text{C}$ with a Skyrme-type ΛN effective interaction. Salcedo and Oset⁷ obtain, for nuclear matter, $\Gamma_{\text{nm}}/\Gamma_n \approx 3$. These calculations are sensitive to the effective weak Hamiltonian and generally have been constrained to satisfy the $\Delta I = \frac{1}{2}$ rule.

We would like to thank Gary Wilkin, Vito Manzella, Ed Meier, and Al Minn for their tireless efforts and help in the construction and installation of much of the equipment used in this experiment. In addition, the assistance of Ed Frank, Tom Holodnik, Michael Vollero, and Judy Twigg is gratefully acknowledged. Finally, the cooperation of the AGS staff is sincerely appreciated. Conversations with C. Dover and A. Gal are gratefully acknowledged. This work has been sup-

ported in part by the U.S. Department of Energy under Contract DE-AC02-76ER0 3244.A012. The work of one of us (B.B.) was supported by Sandia National Laboratory, Albuquerque, New Mexico, through the SURP program. The results presented here constitute part of a thesis to be submitted to Carnegie-Mellon University by one of us (R.G.) in partial fulfillment of the requirements for the Ph.D. degree.

^(a)Present address: Nuclear Physics Laboratory, University of Illinois, Champaign, Ill. 61820.

^(b)Present address: Physics Department, Wheaton College, Wheaton, Ill. 60187.

¹C. B. Dover and G. E. Walker, Phys. Rep. **89**, 2, (1982), and references contained therein.

²B. H. J. McKellar and B. F. Gibson, Phys. Rev. C **30**, 322 (1984).

³C. Y. Cheung, D. P. Heddle, and L. S. Kisslinger, Phys. Rev. C **27**, 335 (1983).

⁴D. P. Heddle, Ph.D. thesis, Carnegie-Mellon University, 1984 (unpublished).

⁵J. Dubach, Bull. Am. Phys. Soc. **27**, 702 (1982).

⁶H. Bandō and H. Tahaki, Prog. Theor. Phys. **72**, 106 (1984); K. Takeuchi, H. Tahaki, and H. Bandō, Prog. Theor. Phys. **73**, 841 (1985); H. Bandō, in Proceedings of the European Symposium on Few-Body Physics: Mesons and Light Nuclei III, Bechyne, Czechoslovakia 27 May–1 June 1985 (to be published).

⁷L. L. Salcedo and E. Oset, to be published.

⁸K. J. Nield *et al.*, Phys. Rev. C **13**, 1263 (1976).

⁹LESBI stands for low-energy separated beam I; see M. Zeller, L. Rosenson, and R. E. Lanou, Jr., Brookhaven National Laboratory Report No. 16000, 1970 (unpublished), p. 193; D. Marlow *et al.*, Phys. Rev. C **25**, 2619 (1982).

¹⁰R. E. Chrien *et al.*, Phys. Lett. **89B**, 31 (1979).

¹¹A. Montwill *et al.*, Nucl. Phys. **A234**, 413 (1974).

¹²T. Cantwell *et al.*, Nucl. Phys. **A236**, 445 (1974).

¹³R. Bertini *et al.*, Nucl. Phys. **A360**, 315 (1981), and **A368**, 365 (1981).

¹⁴T. Aways, Nucl. Instrum. Methods **174**, 237 (1980).